ICCPGE 2016, 1, 25 - 30

Airflow and Heat Transfer by Natural Convection in Small-Scale Vertical Channel

Ahmed Habeb*
[1]Faculty of Engineering and Technology, Sebha University, Brack Alshaty, Libya
*Corresponding Author: a_habeb_71@yahoo.co.uk

Abstract

The natural convection of air in a close-sided vertical channel has been experimentally studied. A laboratory model (height, H=0.1m x width, w=0.1m) with a rectangular cross-section was heated with a uniform heat flux from one side while the other side was kept adiabatic. The experiment was carried out under various operating conditions, variable channel depths (s=45mm, 55mm and 65mm) and variable heat inputs (Qin= 5W, 10W, 20W and 25W). Airflow and heat transfer behaviour was investigated extensively and dimensionless correlations were derived as a function of the modified Rayleigh number (Ra*) and aspect ratio of the channel (s/H).

Keywords: Natural convection; Vvertical channel; air

1. Introduction

Heat transfer by natural convection is a passive phenomenon and therefore an attractive proposition for various applications, in that it requires no mechanical aids. Natural convection airflow along a single vertical plate is one example, applicable in electrical application, e. g. transformers. It is a complex phenomenon depending very much on geometry, among other factors. Even in the case from vertical surfaces, the variations include, for example, a single plate surface or a vertical channel between two plates; open-sided or closed sided channels; and uniform heat flux (isoflux, UHF) or uniform wall temperature (isothermal, UWT).
Wide range of studies concerned with this subject were considered the problem theoretically and experimentally and important correlations were derived, [1-3]. Second example is found in vertical open-ended channels occurs in passive solar air collectors (big-scale channel) such as Trombe wall [4].After the invention of Trombe wall, several studies have focused on studying heat transfer and airflow behaviour inside such aUHF channels. For example, [5,6] who carried out an extensive numerical solution and derived complex correlations for laminar and turbulent flow. Whereas, [7-10] derived empirical correlations based on an indoor experimental data describing airflow and heat transfer for a UHF vertical channels which were more than 1m2 area. Other situations where natural conviction occurs is from cooling fins on electronic equipment (usually in small scale). Since the seminal work of [11], there have been many investigations of buoyancy-driven convection between vertical plates (open-sided and closed sided small scaled-vertical channels). Most of the studies were conducted on water as a working fluid and for a UWT heating mode. In instance,
[12] collected and experimental data and derived correlations for various channel aspect ratios (s/H) and inclinations.[13] also carried out experiments on natural convection in air between two isothermal plates to study the effect of inclination and plate spacing on the behaviour of heat transfer. They observed that the Nu, which describes the heat transfer to fluid, in all cases was dependent on the separation distance between the plates, but not strongly dependent on the plate inclination. Finally, [14] investigated experimentally the

natural convection turbulent airflow between two small vertical plates. The study included both the cases of symmetrically and asymmetrically isothermal heated channels. In the case of symmetrical heating, they observed a high velocity gradient close to the heated plates and a reversed flow at the centre close to the channel entrance. In the second case (asymmetrical heating), the results indicated a large vortex, with an upward flow along the hot plate and downward flow along the cold plate with a wide boundary layer near the hot wall.

This paper reports an experimental work and analysis of data to characterise the heat transfer and airflow within an open-ended vertical small-scaled channel (0.1m x 0.1m) . The model was designed for UHF different heating mode and different channel depths. The aim of the present work is to investigate the effect of the variation of heat input and channel depth on airflow and heat transfer behaviour inside the channel.

2. Experimental Set-Up

The experimental model(Figure 1) comprised a vertical channel, open at top and bottom, and enclosed at both sides. The dimensions of the channel were 10cm high (H) and 10cm wide (w), area 0.01m2. The depth of the channel could be altered, ranging from 45mm to 65mm. One of the channel plate was heated uniformly by electrical resistance with four different values (5W, 10W, 15W and 20W). The opposite plate was made from 2mm aluminium plate placed vertically, opposite to heated plate and thermally insulated of 10mm thermal insulation from outside to reduce thermal losses. The sides of the channel was closed by pair of hard wood of the same thickness of the required depth of the channel. Fine (0.2mm diameter) type T copper constantan thermocouples were inserted within the model to determine temperature at inlet, outlet, heated wall and the opposite wall, as illustrated in Figure 2.1 . The thermocouples in the air stream were placed centrally inside lightweight silvered-radiation shields (made from light plastic pipes), about 2cm long. These were designed specifically to reduce as far as possible any effects on the airflow or temperatures within the channel. A further thermocouple was used to measure ambient temperature.

An Airflow TA-5 hot bead anemometer was used to measure the airflow velocity at the entrance

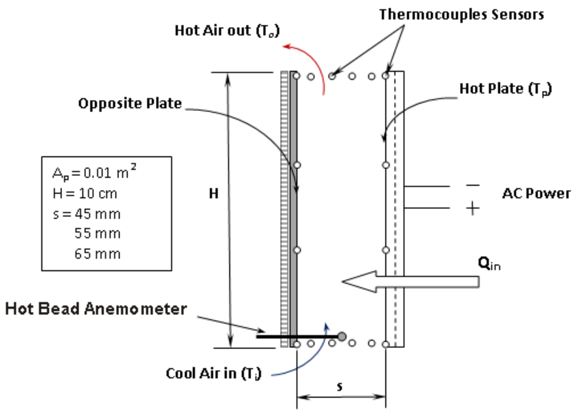

Figure 2.1: Schematic Diagram of the Experimental set-up (not to scale)

of the channel during each experiment. This was provided with an analogue voltage output, which could be recorded by the data logger. The device had been calibrated at BSRIA Instrument Solutions where the accuracy was 0.15 to 1.25m/s, ±(2%, 0.01m/s).

3. Experimental Procedure

In order to achieve accurate results, all thermocouples were calibrated at freezing and boiling points before the commencement the experiment. The standard
deviation of the calibration outcome with 95% confidence gave typically ±0.5°C, and up to ± 0.8°C for the airflow readings, and ± 1.2 °C and ±0.9 °C for the hot
plate and the opposite plate respectively. The propagation rules were used to calculate uncertainties values.

The experimental technique was designed to collect temperatures and velocities taken under several operating conditions, namely different channel depths and different heat inputs. The purpose of these measurements was to study the behaviour of the airflow and heat transfer due to natural convection in a vertical channel. The channel depths tested in this work were 45mm, 55mm and 65mm while the heat inputs were between 5W and 20W at 5W intervals. Each test run started from cold (ambient temperature) and heated at least 2.5 hour, in which the system reached steady state. After each run, the system was allowed to cool down overnight to ensure that the next run

would start again at ambient temperature. Previous researchers experienced some difficulties in measuring the airflow due to air leakage. Therefore, a smoke test was performed at the start of the test sequence to confirm that there was no air escaping from the test rig. The test was carried out after the system had been heating up for about 2.5 hour, and smoke was released at the entrance of the channel while the exit vent was completely sealed. The test did not show any indication of air leakage. Hot bead Anemometer used in the experiment was placed at the entrance of the channel to record the velocity reading (velocity profile assumed to be flat at the entrance) to calculate the mass flow rate afterward. All readings (temperatures and velocities were recorded by a data logger for archiving). All data used in the present work were those obtained at the steady state condition.

4. Results and Discussion

4.1. Transient Response

The transient temperature data closely fit an exponential model of the form:

$$P = P_o\,(1{-}exp(-k't)) \tag{4.1}$$

The asymptote Po from this model was taken as the steady-state value for the purposes of further calculations.A proprietary curve-fitting software package (SigmPolt) was used to fit the data to the requiredexponential curve. From this curve time constants, $(1/k')$ can be derived in accordance with Figure 4.1.
The time constants $(1/k')$, for the overall system, were of the order of 30-70 minutes. For the channel air the typical time constant was about 50minutes, and for the plate and the cover approximately 35minutes. This means the plate and the cover apparently achieve steady state before the airflow. No firm trends were noted for time constants as functions of heat input and channel depth.

4.2. Velocity and Flow Rate

The air velocity profile across the channel was measured, at the bottom, after steady state has been achieved. The velocity profile was fairly flat, as might be expected close to the inlet region, before the hydraulic boundary layers could fully develop, through up the channel. Thus, in order to

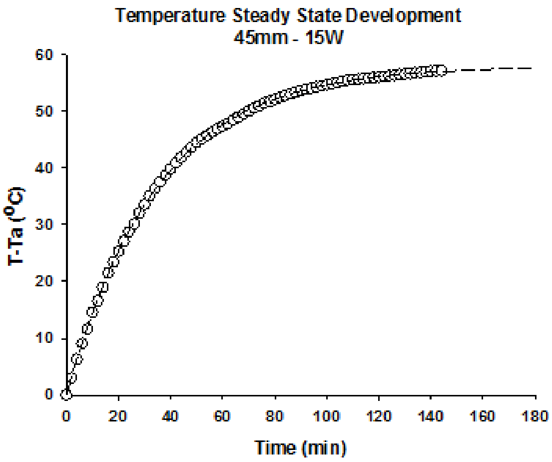

Figure 4.1: Typical Correlation of Hot Plate Temperature against Time

calculate mass flow, the velocity at the bottom was taken as the bulk, or average, velocity. The flow rate is determined by[15]:

$$\dot{m} = \rho_i A_C \bar{u} \tag{4.2}$$

Velocities were observed (see Figure 3a) to increase with increasing heat input. Though the fluid velocity is observed to fall with increasing channel width.However, the mass flow rate increases with increasing channel width and heat input. Typical flow rate range from 0.0013 kg/s (45mm, 5W input) to 0.0022 kg/s (65mm, 20W input). These results are shown in Figure 3b.
Bouchair [10] found that beyond a channel width of 300-500mm (within aspect ratios of 0.2- 0.3), the mass flowrate decreases with increasing channel width. Figure 3b shows no support for these results, in that at low heat inputs and high channel depths, there does not appear to be some levelling off, or even reduction, in flow rates. A numerical analysis conducted by [5] within this range implies an asymptotic straight line beyond a 0.3 aspect ratio (as opposed to a decline).

5. Dimensionless Correlations

The Modified Rayleigh number (Ra") was calculated for all values of channels depths and heat inputs,based on convective heat flux and channel height[1], ranges between 1.6x109 and 4.8 x 109. Ra". Nusselt number , Nu(s), and Reynolds number Re(s) were derived as s function of Ra* and s/H as follows:

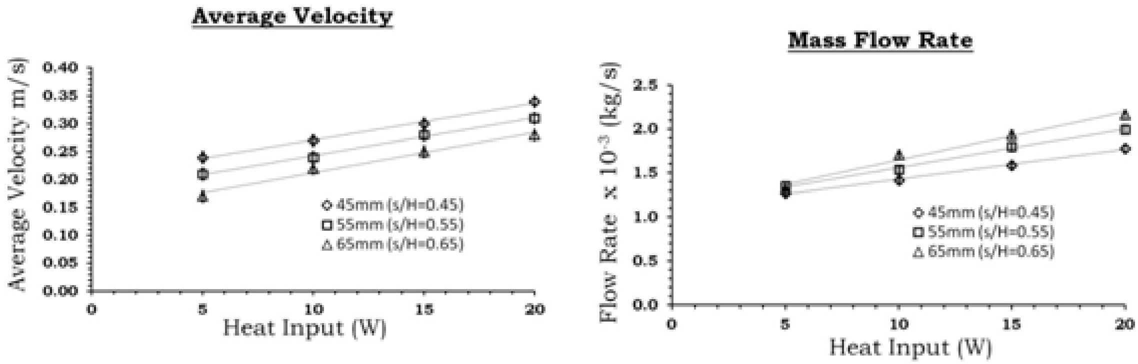

(a) **(b)**

Figure 4.2: Variation of Velocity and Mass Flow Rate with Heat Input

Since:

$$Ra^{*} = \frac{g\beta Q_c H^4}{A_p k v^2} \tag{5.1}$$

and the overall convective coefficient$\bar{h}$ was calculated from:

$$\bar{h} = \frac{Q_c}{A_p\left(T_p - T_m\right)} \tag{5.2}$$

and "Q" _"c" can be calculated fromthe following heat balance :

$$Q_c = \dot{m}C_p T_o - T_i) \tag{5.3}$$

where the heat flux across the glass wall is neglected. In all casesstudied here, the convective coefficient $\bar{h}$ ranges between 4.6 and 11.7 W/m^2K and show slight increase when heat flux increases. This leads to calculated Nu(s) (Nusselt Numberas a function of channel depth (s)) by using the following equation:

$$Nu\left(s\right) = \bar{h}.s/k \tag{5.4}$$

In order to derive a correlation to determine Nu(s) as a function of Ra* and the aspect ratio (s/H), mathematical formula was suggested to take the following form:

$$Nu(s) = a\left[Ra*\right]^{b}\left[s/H\right]^{c} \tag{5.5}$$

Where a, b and c are constants.
Figure 5.1shows Nu(s)plotted against Ra* along with the results of [7,8]. It is clear that Nu(s) increases as the heat input for a given channel depth. By using the standard multiple regression techniques, correlation constants in equation 7 were computed as well as the standard error (S.E) and the correlation coefficient (R^2). This technique was, for example, used by [7-9]. Table 5.1 lists the current results along with the previous results of [7,8] for comparison.

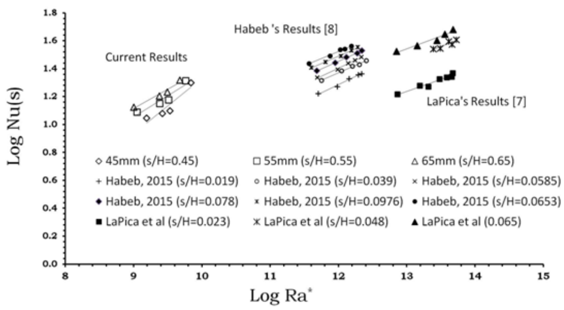

Figure 5.1: Nusselt Number against Rayleigh Number

Table 5.1: Regression Coefficients for Nu(s) against Ra*

Constant	a	b	c	S.E	R^2
Current Results H=0.01m	0.022	0.322	0.783	0.035	0.895
La Pica et al [7]H= 2.6m	0.932	0.203	0.895	0.023	0.98
Habeb [8] H=1.025m	0.19	0.219	0.454	0.008	0.992

In order to study the behaviour of the airflow, Reynolds number, based on the channel depth (s), was used as an indicator. Re(s) was calculated using the following equation [15]:

$$Re(s) = \frac{\bar{u}s}{v} \quad (5.6)$$

Applying a similar technique as above, the following mathematical form suggested here is:

$$Re(s) = a\,[Ra*]^b\,[s/H]^c \quad (5.7)$$

Figure 5.2 presents the relationship between Re(s) and Ra* which can be clearly seen that Re(s) increases as the heat input increases for a given channel depth. Standard multiple regression techniques was used again to evaluate the correlation constants and associate statistical values (S.E and R^2). Table 5.2 lists these values along with results of previous researchers [7,8]also for comparison.

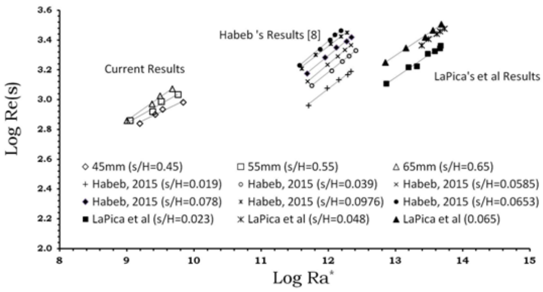

Figure 5.2: Reynolds Number against Rayleigh Number

Table 5.2: Regression Coefficients for Re(s) against Ra*

Constant	A	b	c	S.E	R^2
Current Results(H=0.01m)	4.031	0.265	0.608	0.016	0.964
La Pica et al [7], H= 2.6m	0.501	0.315	0.418	0.011	0.992
Habeb [8] H=1.025m	0.359	0.364	0.626	0.009	0.995

To compare the current results with previous ones, Table 5.1 and Table5.2 show together results from selected previous studies. The current results do not match with previous results. Differences can be attributed to: the extents of the data available for each study; the differences in height of the models; differences in the constructions of the model; differences in locations in measurement points; different flow pattern, and other uncertainties and experimental errors. In instance, turbulent regime of the airflow was detected at the outlet of the channel [7] as the channel height is a strong function of Ra*. Habeb [8] also observed a sign of a turbulent flow byusing a PIV device (Particle Image Velocimetry) particularly at the entrance. However, the slope of the equations (represented by the constant b) show reasonable agreement for Nu(s) and Re(s) equations).

6. Conclusion

The data from this investigation yield some insights into the performance of this kind of application, by varying the heat input and channel depth. The following are the main conclusions from this investigation:

- According to obtained results, the heat transfer coefficient is dependent on the heat input and channel depth. For heat inputs up to 2000W/m^2. The present data gives the following results:

  $$\bar{h}\ is\ proportional\ to\ Q_{in}^{0.322}$$

  and

  $$\bar{h}\ is\ proportional\ to\ S^{0.783}$$

- The mass flow rate within the channel depends on both the heat input and the channel depth. In accordance with Equation 9 and Table 2, the current investigation suggests that:

  $$\dot{m}\ is\ proportional\ to\ Q_{in}^{0.265}$$

  and

  $$\dot{m}\ is\ proportional\ to\ S^{0.608}$$

Other previous results (for example [10]) suggested that there may be an optimum channel depth, which may depend on heat input, to give maximum flow rate.However, data from the current investigation for low heat inputs and at high aspect ratios do not show any support for this assertion.

7. Acknowledgment

This work was conducted within the Mechanical Department at the Faculty of Engineering and Technology - Sebha University. Grateful acknowledgment is presented to whom gave support and consultation.

References

[1] Sparrow, E.M. and Gregg J.L., Laminar Free Convection from a Vertical Plate with Uniform Surface Heat Flux. Transactions of the ASME, (1956), vol. 78, pp. 435-440.

[2] Sparrow, E.M. and Gregg J.L., Similar Solutions for Free Convection from a Non-isothermal Vertical Plate. Transactions of the ASME, (1958), vol. 80, pp. 379-386.

[3] Churchill, S.W. and Chu, H.H.S., Correlating Equations for Laminar and Turbulent Free Convection from a Vertical Plate. International Journal of Heat and Mass Transfer, (1975), vol. 18, pp. 1323-1329.

[4] Duffie, J.A. and Beckman, W.A., Solar Engineering of Thermal Processes. John Wiley & Sons, (2006), ISBN: 0471698679.

[5] Akbari, H. and Borgers, T., Free Convective Laminar Flow Within the Trombe Wall Channel. Solar Energy, (1979), vol. 22, pp. 165-174.

[6] Borgers, T.R. and Akbari, H., Free Convective Turbulent Flow within the Trombe Wall Channel. Solar Energy, (1984), vol. 33, pp. 253-264.

[7] La Pica, A., Rodono, G., and Volpes, R., An Experimental Investigation on Natural Convection of Air in a Vertical Channel. International Journal of Heat and Mass Transfer, (1993), vol. 36, pp. 611-616.

[8] Habeb A.,Buoyancy-Driven Convection in Passive Solar Air Heating Collectors Thesis (PhD), (2014), SEBE, Glasgow Caledonian University.

[9] Burek, S. and Habeb, A., Air Flow and Thermal Efficiency Characteristics in Solar Chimneys and Trombe Walls. Energy and Buildings, (2007), vol. 39, pp. 128-135.

[10] Bouchair, A., Solar Chimney for Promoting Cooling Ventilation in Southern Algeria. Building Services Engineering Research and Technology, (1994), vol. 15(2), pp. 81-93.

[11] Elenbaas, W., Heat Dissipation of Parallel Plates by Free Convection. Physica, (1942), vol. 9. Pp. 1-24.

[12] Azevedo, L.F.A. and Sparrow, E.M., Natural Convection in Open-Ended Inclined Channels. Journal of Heat Transfer, (1985), vol. 107, pp. 893-901.

[13] Onur, N. and Aktas, M., An Experimental Study on the Effect of Opposing Wall on Natural Convection along an Inclined Hot Plate Facing Downward. International Communications in Heat and Mass Transfer, (1998), vol. 25, pp. 389-397.

[14] Habib, M.A., Said, S.A.M. and Asghar, A.A., Velocity Characteristics of Turbulent Natural Convection in Symmetrically and Asymmetrically Heated Vertical Channels. Experimental Thermal and Fluid Science, (2002), vol. 26. pp. 77-87.

[15] Incropera, F.P. and Dewitt, D.P., Fundamentals of Heat and Mass Transfer. USA, John Wiley & Sons, (2002), ISBN: 0471386502.